IEEE Access
Multidisciplinary | Rapid Review | Open Access Journal

Received October 15, 2020, accepted October 19, 2020, date of publication October 26, 2020, date of current version November 9, 2020.

Digital Object Identifier 10.1109/ACCESS.2020.3033524

UAV-Assisted Relaying Transmission Design and Optimization for High-Speed Moving Sources

JI WU, LIHUA LI, (Member, IEEE), AND LIUTONG DU, (Student Member, IEEE)
State Key Laboratory of Networking and Switching Technology, Beijing University of Posts and Telecommunications, Beijing 100876, China
Corresponding author: Lihua Li (lilihua@bupt.edu.cn)

This work was supported by a grant from the National Key Research and Development Program of China under Grant 2018YFF0301201.

ABSTRACT In state of the art relay-assisted transmission schemes, analysis of symbol error ratio (SER) and throughput mainly focuses on static or low-speed sources, where relay strategies and power allocation strategies are studied. However, when the sources move quickly with variable trajectories, the power allocation strategy of relays is affected by the sources' movement and time-varying channels, and should be adjusted dynamically according to the sources' trajectories with corresponding motion scenarios. Therefore, previous schemes are no longer applicable to solve the problem brought by high-speed sources because their channels and power allocation strategies are lack of correlation with the sources' movement. In this article, taking full advantage of the flexibility of unmanned aerial vehicle (UAV) combined with multi-antenna technology, we propose two UAV-assisted relaying transmission schemes to serve high-speed moving sources. Through derivation and optimization of system's symbol error ratio (SER), new dynamic power allocation and adjustment strategies of the source and each UAV are obtained when the total power of the system is limited. Moreover, the proposed schemes utilize time-based power allocation lists to save signaling overhead. Simulation results demonstrate that our schemes outperform the compared schemes.

INDEX TERMS Moving sources, UAV relays, dynamic power allocation.

I. INTRODUCTION

A. MOTIVATION AND RELATED WORKS

In wireless communication, especially when the conditions of communication equipment are limited or the communication environment is poor, relay-assisted end-to-end signal transmission can effectively suppress the effect of fading and ensure reliable communication. Various types of relay devices have been adopted, including base stations (BSs), stationary repeaters, or mobile devices. Amplify Forwarding (AF) and Decode Forwarding (DF) are two of the most popular relay protocols. Reference [1] studies the performance of a OFDM-based AF relay system. In [2], DF relay system's performance in κ-μ and η-μ fading channels is evaluated in detail. Moreover, hybrid AF and DF relay system is proposed in [3], where the author adopts Non-Orthogonal Multiple Access (NOMA) to obtain larger average system throughput with higher complexity than either AF scheme or DF scheme. Although DF relay strategies always have a better performance compared with AF ones due to decoding and re-encoding, AF strategies are more widely adopted because of lower complexity and implementation cost.

Based on these cooperative relaying protocols, performance of traditional stationary relay system including bit error ratio (BER) and outage probability have been well evaluated in [4]–[14], moreover, power allocation strategies have also been proposed. However, all these schemes have their shortages. Specifically, [4] has deduced and analyzed the outage probability of traditional static multi-point AF relay system with a single antenna, [5] compares the outage performance of AF and DF systems. Reference [6] studies average BER performance and resource allocation strategies in DF stationary relay system with limited power, while [7] focuses on the comparision of BER performance of the two stationary systems. In addition, [8]–[10] propose different power allocation strategies in stationary relay systems with a single atenna. In detail, in [8], power allocation and relay selection of AF relay system with single antenna at each end are jointly optimized in order to minimize system BER, but the end-to-end distances are fixed. Based on system SNR, [9] proposes a multi-relay cooperative transmission scheme with a single antenna. The power allocation strategy and the distance between each end are variable, but this article considers

The associate editor coordinating the review of this manuscript and approving it for publication was Ahmed F. Zobaa.

the power at each end and the change of the end-to-end distance as two types of unrelated variables. Specific study of the optimal power allocation scheme of AF relay system under power limitation is shown in [10]. Although multiple relays are used, the transmission and reception of each end is still equipped with a single antenna, causing the shortage of the diversity gain. In summary, these performance analysis and power allocation strategies are all based on a single antenna for simplicity, which can hardly meet the challenge of the future communication in the fifth generation (5G) era. Moreover, these stationary schemes do not consider the high-speed mobility of the sources and the relays.

Taking the limitations of a single antenna into consideration, multi-relay cooperative transmission schemes combined with multiple input and multiple output (MIMO) technology have attracted more attention due to its diversity gain. Reference [11] studies the application of MIMO precoding in AF relay system, proving that additional links can effectively expand the coverage of multi-hop network. Reference [12] analyzes the improvement of BER performance of AF relay cooperative system combined with MIMO, however, it still does not consider the mobility of each end. Reference [13] combines relay system with energy harvesting, two antennas are used at the source, but only one antenna with the best performance is chosen for transmission and this scheme has not considered the high-speed movement of the source. As shown in [14], energy harvesting is performed at the relay first, then time splitting ratio (TSR) and power splitting ratio (PSR) strategies are adopted in multi-antenna-based AF system respectively, but the mathematical relationship between PSR and the end-to-end distance as well as the trajectory of the source is not emphasized. Although multiple antennas are adopted, the above papers are mainly based on stationary relays and sources, so their power allocation schemes are not strongly related to real-time channel conditions, causing limited flexibility.

Even the mobility of the source is well considered, traditional relay devices still limit the flexibility of these schemes because stationary relays have difficulty in flexible placement and adjustment according to the source's movement. Fortunately, UAV relays meet the demand perfectly. Thanks to its exquisite design and versatility, UAV is widely used as a new kind of relay to assist communication. Advantages brought by UAVs' mobility and capabilities of flexible adjustment and deployment, public safety problems of UAVs and UAV relaying schemes have been discussed in [15]–[27].

Firstly, height, a new dimension of variable introduced by UAV relays provides new ideas in relays' placement and the optimization of the above-mentioned traditional relaying schemes. In [15], in contrast with traditional ground facilities, aerial UAVs can be dynamically adjusted according to real-time requirements with flexible deployment. In addition, due to UAVs' high and controllable 3D mobility, the flight trajectories are more suitable for more complex and changeable scenes. In [16], benefited from line-of-sight dominant channel, the arrangement of UAV relays can generally reduce the effect of fading, thereby gaining better link quality and higher reliability. In [17], UAV's height and path loss compensation factor are jointly optimized in order to obtain better coverage and throughput performance, in which transmit power of UAV is also optimazed. In brief, the height of UAVs as well as their 3D mobility is of great significance that can be utilized in relay systems and corresponding power allocation strategies.

Also, UAV relays are well discussed in public safety communications, including signal transmission security, public application safety and hardware safety. Specifically, in [18], UAV assisted secure transmission for scalable videos in hyper-dense networks via caching is studied. Through pre-caching, the precoding matrices of small-cell base stations (SBSs) based on interference alignment are designed cooperatively to disrupt eavesdropping. Reference [19] proposed a novel scheme to guarantee the security of UAV-relayed wireless networks with caching via jointly optimizing the UAV trajectory and time scheduling. In brief, caching UAVs can not only ensure transmission security but also save signaling overhead to some extent becaused pre-caching in UAV can reduce the cost of resource loading and scheduling. Authors in [20] propose a multi-layered network architecture incorporating UAVs for public safety communication with taking into accounting the energy consumption criteria. Collision avoidance, trajectory optimization, recharging automation, energy efficiency and other perspectives on UAV deployment and endurance are comprehensively discussed. So the UAV's safety must be well considered in the design of the UAV-assisted relaying system.

Moreover, combining AF relay strategies with UAV technology, [21]–[24] have discussed the improvement of system performance including energy efficiency and spectrum efficiency and the optimization of energy. Reference [21] introduces the connection strategy and channel characteristics of cooperative UAVs and traditional communication network. On this basis, [22] studies the improvement of energy efficiency and spectrum efficiency of mobile UAVs in traditional system, [23] studies the trajectory design and energy optimization problem of UAV relaying system which serves multiple users. In addition, authors in [24] propose power headroom report-based power efficient resource allocation (PHR-PERA) scheme to adjust user uplink power and improve throughput, which has made excellent contribution in power control and can be applied to UAV-assisted relaying systems.

In addition, power allocation strategies in UAV-assisted relaying systems are proposed in [25]–[27]. In detail, [25] proposes that in the UAV-assisted IoT network, TSR and PSR strategies are widely used for multi-UAV relaying transmission. However, power splitting ratio in this article adopts only a few discrete samples, making these strategies not universal enough to meet the need of the continuously changing trajectories of the source. In [26], the author analyzes the SER performance of the UAV relaying system with energy harvesting under the two-path fluctuating channels,

but this article obtains better SER performance by changing the power allocation factor, rather than establishing a SER optimization goal and solving the problem to get the corresponding optimal power allocation strategy. Authors in [27] analyze a novel relaying scheme named as incremental hybrid decode-amplify-forward relaying (IHDAF), in which they have derived the closed-form expressions of BER and discussed its optimal performance when distance between each end changes, the power allocation factor changes in the meanwhile. These schemes have considered that power allocation strategies should be changed according to the end-to-end distance and some other factors, but they ignore the continuous relevance of the power allocation and the factors. Discrete samples can not perfectly meet the need of power adjustment, because in the UAV-assisted relaying system with high-speed moving sources, continuous adjustment of power allocation shoule be adopted in order to meet the challenge of the time-varying channels.

B. OUR CONTRIBUTIONS AND ORGANIZATION

A considerable percentage of existing AF relay schemes are based on single-antenna sources and relays, the gain of which is apparently limited. In the meanwhile, the anti-fading ability is not strong enough in the communication scenario where the source's motion state changes rapidly. As a result, system performance like SER will be greatly restricted.

In existing multi-relay schemes, in view of low implementation cost, fixed power allocation strategies are mainly adopted. In addition, stationary relays have limited flexibility and are hard to cope with high-speed variable channels. As for dynamic power allocation in existing UAV relaying schemes, because less consideration is given to the high-speed movement of the source, they are not suitable for practical scenarios, and traditional adaptive power control strategy has signaling overhead.

In view of these limitations, we have proposed targeted schemes which are suitble for AF relay systems to serve high-speed sources. For clarity, We summarize the contributions of our paper as follows:

- A motion scenario with fast time-varying channels is adopted, in which the total power of the system is limited. In addition, due to environmental influences and limitations of transmitter hardware, the signal from the moving source can only be transmitted with quite limited power.
- A new multi-antenna AF relay scheme with multiple UAVs is proposed to assist the transmission for high-speed moving sources. In detail, the multiple UAVs will be used as hovering relays for cooperative transmission and corresponding expressions are presented.
- A new single-UAV relaying scheme is proposed to assist the transmission for high-speed moving sources in which two different situations are discussed. For one, the UAV relay perfectly following the moving source with the same trajectory during the whole motion. For another, the following UAV can not keep up with the moving source from a specific moment which results in different trajectories of the UAV and the source. Related analysis and expressions are also presented.
- Optimization functions based on system SER minimization of the above two schemes are proposed respectively. Through derivation and calculation of the formulas in these two schemes, corresponding dynamic power allocation strategies are obtained finally which are able to cope with the problems caused by the moving source. Due to the power adjustment lists, no signaling overhead of the source and the UAV are required.

Simulation results demonstrate that our schemes have lower SER during the whole process of motion. Dynamic adjustment of each end's power can be recorded or cached in a timetable according to the source's predictable trajectory to reduce the signaling overhead. Furthermore, simulations show that the optimal number of UAVs suitable for each scenario is variable, which has great value for further research.

The rest of the paper is organized as follows. The system models of the two schemes are proposed in Section II. In Section III and IV, we respectively carry out derivation and calculation of the formulas, and get the expression of SER and power allocation of both multi-UAV scheme and single-UAV scheme. Simulations and analysis are presented in Section V. Finally, we conclude this article in Section VI.

C. NOTATIONS

In this article, the following notations will be adopted. Matrices will be presented by boldface uppercase letters. $\|\mathbf{A}\|_{\mathbf{F}}$ denotes the Frobenius norm of matrix $\mathbf{A}$, $(\mathbf{A})^{\mathbf{T}}$ denotes the transpose matrix of $\mathbf{A}$, $|\mathbf{x}|$ denotes the modulo operation of vector $\mathbf{x}$. $|E|$ stands for the absolute value of E which is digital formula. In addition, $(\cdot)^*$ denotes the conjugate operation. $Q(x)$ denotes the Q-function.

II. SYSTEM MODELS

In this section, system models of the two UAV relaying schemes are presented. Multiple hovering UAVs at reasonable locations are used as relays in one scheme, and dynamic power allocation is carried out to assist the multi-hop transmission from a high-speed moving source to BS. Moreover, in another scheme, a single UAV is used as mobile relay to follow the moving source. System models of these two schemes will be illustrated respectively.

A. MULTIPLE HOVERING UAVS ASSISTED TRANSMISSION

As shown in Fig. 1, a typical motion scene is placed in the Cartesian coordinate system. As indicated by the red dotted arrow at the source which stands for the direction of movement, the source moves down the surface of the slope quickly. a denotes the fixed acceleration. We assume that the slope is approximately a straight line and the height drop is H, the horizontal length is L and the tilt angle is θ. The coordinates of the source are written as functions of time

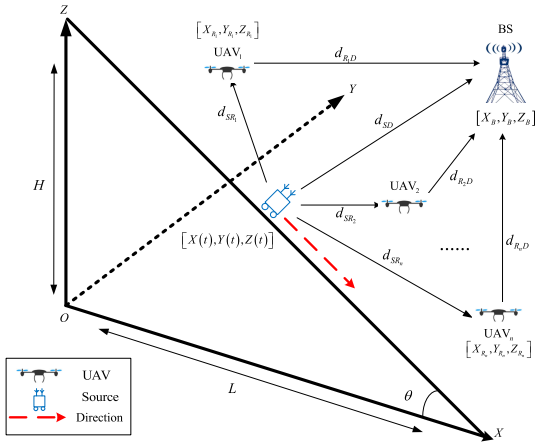

FIGURE 1. System model: Multiple hovering UAV relays assist for high-speed moving source in multi-point and multi-hop transmission system.

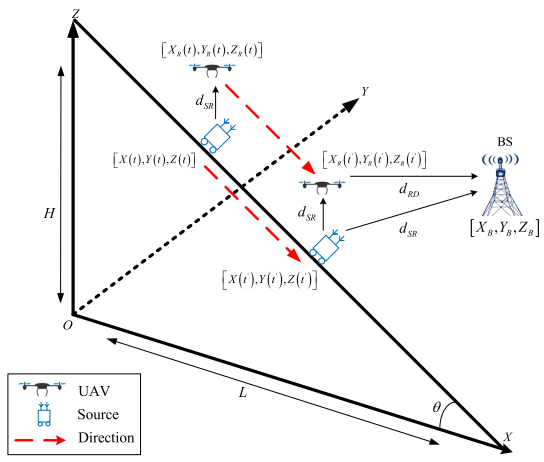

FIGURE 2. System model: Single mobile UAV relay assists for high-speed moving source by following it in multi-hop transmission system.

t according to its specific motion trajectory, expressed as $[X(t), Y(t), Z(t)]$. The coordinates of BS is $[X_B, Y_B, Z_B]$.

n UAVs are deployed in this model. According to the scenario, the optimal position of the ith hovering UAV is fixed as $\left[X_{R_i}, Y_{R_i}, Z_{R_i}\right], i \in (1, n)$ in advance and can be adjusted when the scenario and source's movement change. We assume that each UAV is located directly above the source's trajectory, in this way, Y_{R_i} can be regarded as 0 for simplicity. d_{SD} denotes the distance between the source and BS, d_{SR_i} denotes the distance between the source and the ith UAV relay, d_{R_iD} denotes the distance between the ith UAV and BS. In addition, these end-to-end distance arrows also represent the signal transmission direction of each link.

Due to the limitations of light UAV's carrying capacity, the STBC dual antennas transmission scheme is adopted as the standard for the source in this article. The UAV relays use 2 antennas for transmission and a single antenna for reception. In addition, the remote BS equips with M receive antennas. The channel from the source to BS and the channels from each UAV to BS, expressed as $\mathbf{H}_{SD}, \mathbf{H}_{R_iD}$, are both $M \times 2$ matrices. $\mathbf{H}_{SR_i}$ denotes the channel matrix from the source to the ith UAV relay whose dimension is 1×2. Three types of links are shown in Fig. 1.

B. SINGLE FOLLOWING UAV ASSISTED TRANSMISSION

Different from the multi-UAV scheme, the single-UAV will be no longer restricted by the safe distance between adjacent UAVs, therefore, a more flexible following strategy will be adopted. As is illustrated in Fig. 2, only the number of UAV as well as the UAV's placement changes, while other conditions of the scenario remain the same. Owing to UAV's movement, we consider two different situations.

Since the standard of light UAVs stipulates that the maximum moving speed of UAV cannot exceed 28m/s, in the first situation, we assume that the maximum speed of the source is less than this limitation, which means the UAV can perfectly follow the trajectory of the source during the entire moving process. In this way, the UAV and the source move in a same mode. The real-time coordinates of the UAV can be written as $[X_R(t), Y_R(t), Z_R(t)]$, influenced by specific motion state of the source. For example, when motion time is t', the UAV's position and coordinates change accordingly as Fig. 2 shows.

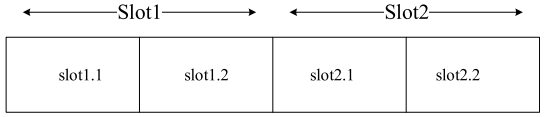

FIGURE 3. Time slot distribution diagram of a complete group of signal transmission.

However, the larger scene and longer motion time may lead to another situation where the UAV reaches the maximum speed at a certain moment and can no longer keep up with the source which is still accelerating. In fact, this situation is more common so we can divide the total motion time into 2 parts, including the $0 - t_1$ period in which the UAV can perfectly follow the source at the same speed, and the $t_1 - t_2$ period in which the UAV reaches its velocity limitation. Relative speed between the UAV and the source exists during $t_1 - t_2$, causing different motion trajectories.

III. PROBLEM FORMULATION OF MULTIPLE HOVERING UAVS SCHEME

A. MULTI-HOP SIGNAL TRANSMISSION EXPRESSION

As for a two-hop relay system, in the first slot called Slot1, the source sends signals to BS and to each UAV simultaneously. In the second slot called Slot2, each UAV will amplify the received signal from Slot1 and forward to BS. In the end, BS performs maximum ratio combining (MRC) on the signal from the source and that from each UAV relay.

As is illustrated in Fig. 3, with STBC strategy, Slot1 is divided into two small time slots named Slot1.1 and Slot1.2.

Taking the jth $(1 \leq j \leq M)$ receiving antenna of BS as an example, signal x_1 is transmitted from the first antenna of the source in slot1.1, and signal x_2 is transmitted from the second antenna at the same time. The received signal at BS at this moment is written as:

$$y_{SD_j}(1) = \sqrt{P_S}\left(h_{SD}^{1,j}x_1 + h_{SD}^{2,j}x_2\right) + n_j(1) \tag{1}$$

where P_S denotes the transmission power of the source, $h_{SD}^{1,j}, h_{SD}^{2,j}$ denotes the channel coefficients of the two antennas from the source to the jth antenna at BS respectively. $n_j(m)$ denotes the additive noise, $m = 1, 2$.

Next, $-x_2^*$ is transmitted from the first antenna in slot1.2 and x_1^* is transmitted from the second antenna as well. So the received signal at BS in slot1.2 can be written as:

$$y_{SD_j}(2) = \sqrt{P_S}\left(-h_{SD}^{1,j}x_2^* + h_{SD}^{2,j}x_1^*\right) + n_j(2) \tag{2}$$

Linearly combing the signals of two time slots, we can get the final signal expression in Slot1:

$$y_{SD}(m) = \sum_{j=1}^{M}\sqrt{P_S}\sqrt{\left|h_{SD}^{1,j}\right|^2 + \left|h_{SD}^{2,j}\right|^2}x(m) + n_j(m) \tag{3}$$

where $m = 1, 2$.

In the two-hop relay system, the received vector at the BS in Slot1 is as follows:

$$\mathbf{y}_{SD} = \sqrt{P_S}\cdot\mathbf{H}_{SD}\cdot\mathbf{x} + \mathbf{n}_{SD} \tag{4}$$

where $\mathbf{y}_{SD}$ is the $M \times 1$ vector, $\mathbf{x}$ is the transmitted vector, and $\mathbf{n}_{SD}$ is the $M \times 1$ additive noise vector, whose elements are $i.i.d.\ \mathcal{CN}\left(0, \sigma_0^2\right)$. $\mathbf{H}_{SD}$ denotes the channel matrix from the source to the BS, which can be formed by stacking the channel vector of each transmit antenna as $\mathbf{H}_{SD} = [\mathbf{h}_{SD}^1, \mathbf{h}_{SD}^2]$. Channel vector of each transmit antenna at the source is denoted as $\mathbf{h}_{SD}^p = [\mathbf{h}_{SD}^{p,1}, \ldots, \mathbf{h}_{SD}^{p,q}, \ldots, \mathbf{h}_{SD}^{p,M}]^{\mathbf{T}}$, $p = 1, 2$, and $q \in (1, M)$. In detail, $h_{SD}^{p,q}$ denotes the channel coefficient from the pth transmit antenna at the source to the qth receive antenna at the BS.

The transmission from the source to the ith UAV in Slot1 is consistent with the process of the direct link between the source and BS in principle, which can be written as:

$$y_{SR_i}(m) = \sqrt{P_S}\sqrt{\left|h_{SR_i}^1\right|^2 + \left|h_{SR_i}^2\right|^2}x(m) + n_j(m) \tag{5}$$

where $h_{SR_i}^1, h_{SR_i}^2$ denotes the channel coefficients of the two antennas from the source to the ith UAV respectively. In the meanwhile, the received signal at the ith UAV in Slot1 is written as:

$$y_{SR_i} = \sqrt{P_S}\cdot\mathbf{H}_{SR_i}\cdot\mathbf{x} + n_{SR_i} \tag{6}$$

where n_{SR_i} is $\mathcal{CN}\left(0, \sigma_0^2\right)$. $\mathbf{H}_{SR_i}$ denotes the channel matrix from the source to the ith UAV, which can be written as $[\mathbf{h}_{SR_i}^1, \mathbf{h}_{SR_i}^2]^{\mathbf{T}}$.

Similarly, in Slot2, the multiple UAVs will forward the signal based on AF strategy in the relay links between UAVs and BS. In detail, Slot2 is divided into slot2.1 and slot2.2 to fit the STBC strategy, and in this way, the second hop of the whole system has done. At the BS, the received vector in Slot2 is given by:

$$\mathbf{y}_{R_iD} = \lambda_i\cdot\sqrt{P_i}\cdot\mathbf{H}_{R_iD}\cdot\mathbf{y}_{SR_i} + \mathbf{n}_{R_iD} \tag{7}$$

where $\mathbf{y}_{R_iD}$ is the $M \times 1$ vector, $\mathbf{n}_{R_iD}$ is the $M \times 1$ additive noise vector, whose elements are $i.i.d.\ \mathcal{CN}\left(0, \sigma_0^2\right)$. $\mathbf{H}_{R_iD}$ denotes the channel matrix from the ith UAV to the BS, which has the same dimensions and similar definition with $\mathbf{H}_{SD}$, however, its element $h_{R_iD}^{p,q}$ denotes the channel coefficient from the pth transmit antenna at the ith UAV to the qth receive antenna at the BS. P_i denotes the forward transmission power of the ith UAV relay and λ_i denotes the amplification factor, and can be defined as:

$$\lambda_i = \sqrt{\frac{1}{P_S\cdot\left\|\mathbf{H}_{SR_i}\right\|_{\mathbf{F}}^2 + \sigma_0^2}} \tag{8}$$

B. CALCULATION OF SNR AND SER

When adopting MRC at the BS, according to the equivalent transmission model in [28], the link with a larger instantaneous SNR will have a higher weight in the linear combination. Moreover, if the noise of all the links have the same variance, the total SNR can be expressed as the sum of each link's SNR. So we unify the noise of both the direct link and the relay links, where the normalized noise is defined as $n_{nor} \sim \mathcal{CN}\left(0, \sigma^2\right)$.

On the basis of the analysis in Part A, SNR of the direct link can be reasonably derived and written as:

$$\gamma_{SD} = \frac{P_S\left\|\mathbf{H}_{SD}\right\|_{\mathbf{F}}^2}{\sigma^2} \tag{9}$$

In addition, SNR of the relay links can be expressed as:

$$\gamma_{R_iD} = \frac{\frac{P_S\left\|\mathbf{H}_{SR_i}\right\|_{\mathbf{F}}^2}{\sigma^2}\frac{P_i\left\|\mathbf{H}_{R_iD}\right\|_{\mathbf{F}}^2}{\sigma^2}}{\frac{P_S\left\|\mathbf{H}_{SR_i}\right\|_{\mathbf{F}}^2}{\sigma^2} + 1 + \frac{P_i\left\|\mathbf{H}_{R_iD}\right\|_{\mathbf{F}}^2}{\sigma^2}} \tag{10}$$

Above all, the total SNR of the system is defined as:

$$\gamma_{AF}^{MRC} = \gamma_{SD} + \sum_{i=1}^{n}\gamma_{R_iD} \tag{11}$$

In order to simplify matrix calculations, we reckon that $h_{SD}^{p,q}$, follow Rayleigh fading distribution. With the same method as in [27], in this article, we adopt that $E(|h_{SD}^{k,j}|^2) = \sigma_{SD}^2$. σ_{SD}^2 is related to $d_{SD}^{-\alpha}, \alpha \in (2, 4)$, which captures the effect of the path loss on SER. α denotes the fading factor and d_{SD} denotes the real-time distance between the moving source and the remote BS. The same is true for other channels like $\mathbf{H}_{R_iD}$ and $\mathbf{H}_{SR_i}$.

As is depicted in Fig. 1, assuming that the source almost performs uniformly accelerated linear motion, we can easily

obtain that:

$$d_{SD}(t) = \sqrt{\begin{array}{l}\left(X_B - \frac{1}{2}at^2\cos\theta\right)^2 + {Y_B}^2 \\ +\left(H - \frac{1}{2}at^2\sin\theta - Z_B\right)^2\end{array}} \tag{12}$$

$$d_{SR_i}(t) = \sqrt{\begin{array}{l}\left(X_{R_i} - \frac{1}{2}at^2\cos\theta\right)^2 + \\ \left(H - \frac{1}{2}at^2\sin\theta - Z_{R_i}\right)^2\end{array}} \tag{13}$$

where a denotes the acceleration.

According to the characteristics of (9) and (10) and the probability theory, we obtain $\gamma_{SD} \sim E(\beta)$ with parameter β that can be written as:

$$\beta = \frac{\sigma^2}{G_{SD} \cdot P_S \cdot \sigma_{SD}^2} \tag{14}$$

As for γ_{R_iD}, it can be abstracted as the form of $\frac{xy}{x+y+1}$, and it is worth noting that both x and y obey exponential distribution. Calculating in this way, we approximately obtain $\gamma_{R_iD} \sim E(\theta_i)$ with parameter θ_i, which is given by:

$$\theta_i = \frac{\sigma^2}{G_{SR_i} \cdot P_S \cdot \sigma_{SR_i}^2} + \frac{\sigma^2}{G_{R_iD} \cdot P_{R_i} \cdot \sigma_{R_iD}^2} \tag{15}$$

where $G_{SD} = G_{R_iD} = 2M$, $G_{SR_i} = 2$ and $\sigma_{SR_i}^2, \sigma_{R_iD}^2, \sigma_{SD}^2$ in this article can be written as $d_{SR_i}^{-\alpha}, d_{R_iD}^{-\alpha}, d_{SD}^{-\alpha}$, respectively.

Motivated by [29] and [30], we are able to derive the distribution of γ_{AF}^{MRC}, which denotes the sum of several exponentially distributed variables. Based on the above analysis, calculations and mathematical characteristics of γ_{SD} and γ_{R_iD}, we can obtain the probability density function (PDF) of γ_{AF}^{MRC}:

$$\begin{aligned} & f_{\gamma_n}(\gamma) \\ & = \beta\cdot\theta_1\cdot\theta_2\ldots\cdot\theta_n \left[\begin{array}{l} \dfrac{e^{-\beta\gamma}}{\prod_{i=1}^{n}(\theta_i-\beta)} - \dfrac{e^{-\theta_1\gamma}}{\prod_{i=2}^{n}(\theta_i-\theta_1)(\theta_1-\beta)} \\ + \dfrac{e^{-\theta_2\gamma}}{\prod_{i=3}^{n}(\theta_i-\theta_2)(\theta_2-\theta_1)(\theta_1-\beta)} \\ +\ldots+(-1)^n\dfrac{e^{-\theta_n\gamma}}{\prod_{j=1}^{n-1}(\theta_n-\theta_j)(\theta_n-\beta)} \end{array}\right] \end{aligned} \tag{16}$$

γ in (16) denotes γ_{AF}^{MRC} for simplicity.

According to the PDF of γ_{AF}^{MRC} in (16), SER of the multi-UAV relay system can be given as:

$$P_{e_n} = \int_0^\infty Q\left(\sqrt{2\gamma}\right)\cdot f_{\gamma_n}(\gamma)\,d\gamma \tag{17}$$

Finally, with the combination of (16) and (17), SER of the entire scenario is derived as:

$$\begin{aligned} P_{e_n} = & \left(\frac{1}{2} - \frac{1}{2\sqrt{\beta+1}}\right)\cdot\frac{\theta_1\cdot\theta_2\cdot\ldots\theta_n}{\prod_{i=1}^{n}(\theta_i-\beta)} \\ & - \left(\frac{1}{2} - \frac{1}{2\sqrt{\theta_1+1}}\right)\cdot\frac{\beta\cdot\theta_2\cdot\ldots\theta_n}{\prod_{i=2}^{n}(\theta_i-\theta_1)(\theta_1-\beta)} \\ & +\ldots+(-1)^n\left(\frac{1}{2} - \frac{1}{2\sqrt{\theta_n+1}}\right) \\ & \cdot\frac{\beta\cdot\theta_1\cdot\ldots\theta_{n-1}}{\prod_{j=1}^{n-1}(\theta_n-\theta_j)(\theta_n-\beta)} \end{aligned} \tag{18}$$

Equation (17) and (18) are based on the BPSK modulation. Similarly, when higher order modulation of PSK is adopted, (17) and (18) will change accordingly. According to [31], SER of the NPSK modulation system in this scenario will be approximately expressed as:

$$\begin{aligned} & P_{e_n}^{(N)} \\ & \approx 2\cdot\left[\begin{array}{l} \left(\frac{1}{2} - \frac{\sin\left(\frac{\pi}{N}\right)}{2\sqrt{\beta+\sin^2\left(\frac{\pi}{N}\right)}}\right)\cdot\frac{\theta_1\cdot\theta_2\cdot\ldots\theta_n}{\prod_{i=1}^{n}(\theta_i-\beta)} \\ - \left(\frac{1}{2} - \frac{\sin\left(\frac{\pi}{N}\right)}{2\sqrt{\theta_1+\sin^2\left(\frac{\pi}{N}\right)}}\right)\cdot\frac{\beta\cdot\theta_2\cdot\ldots\theta_n}{\prod_{i=2}^{n}(\theta_i-\theta_1)(\theta_1-\beta)} \\ +\ldots+\left(\frac{1}{2} - \frac{\sin\left(\frac{\pi}{N}\right)}{2\sqrt{\theta_n+\sin^2\left(\frac{\pi}{N}\right)}}\right) \\ \cdot\frac{(-1)^n\beta\cdot\theta_1\cdot\ldots\theta_{n-1}}{\prod_{j=1}^{n-1}(\theta_n-\theta_j)(\theta_n-\beta)} \end{array}\right] \end{aligned} \tag{19}$$

where N denotes the modulation order of PSK, $N > 2$.

C. OPTIMIZATION FUNCTION OF SER

In the proposed scenario, high drop and the influence of obstacles lead to the limitation of maximum power of the whole system. The hardware limitations of the source also leads to the low transmit power. Under the condition that the total power of system P_t is limited, reasonable relay arrangement and power allocation strategies are performed to optimize SER. Then the optimization of this scheme can be formulated as follows:

$$\begin{aligned} \min_{P_S,P_1,P_2\ldots P_n} \quad & P_{e_n} = F(P_S, P_1, P_2\ldots P_n) \\ & \mathrm{C1}: P_S + \sum_{i=1}^{n} P_i = P_t \\ \text{s.t.} \quad & \mathrm{C2}: P_S > 0, P_i > 0, i \in (1, n) \\ & \mathrm{C3}: P_S < P_t, P_i < P_t, i \in (1, n) \end{aligned} \tag{20}$$

Based on the optimization problem, the Lagrange multiplier method is appropriately adopted to find a group of approximate optimal solutions.

D. POWER ALLOCATION STRATEGY

The calculation method of the power allocation strategies of BPSK and NPSK are similar in (20). Due to the large number of variables involved, it is extremely difficult to obtain an accurate optimal solution to this problem. However, by making reasonable approximation according to the magnitude of each variable in the practical movement process, we can obtain a group of approximate optimal solutions as:

$$P_i = P_S \cdot \frac{\sigma_{SR_i}^2}{\sigma_{R_iD}^2} \cdot \sqrt{\frac{\left|\left(\sigma_{R_iD}^2 - \sigma_{SD}^2\right)\right| \cdot G_{SR_i}}{\left(G_{SD} \cdot \sigma_{SD}^2 + G_{SR_i} \cdot \sigma_{SR_i}^2\right)}} \tag{21}$$

$$P_S = \frac{P_t}{1 + \sum_{i=1}^{n} \frac{\sigma_{SR_i}^2}{\sigma_{R_iD}^2} \cdot \sqrt{\frac{\left|\left(\sigma_{R_iD}^2 - \sigma_{SD}^2\right)\right| \cdot G_{SR_i}}{\left(G_{SD} \cdot \sigma_{SD}^2 + G_{SR_i} \cdot \sigma_{SR_i}^2\right)}}} \tag{22}$$

By substituting (21) and (22) into (18), the real-time SER of the entire motion process can be calculated.

Noting that $\sigma_{SR_i}^2, \sigma_{SD}^2$ are related to $d_{SR_i}^{-\alpha}, d_{SD}^{-\alpha}$, which are expressed as functions of the time-varying distances of both the direct link and the relay links, so both P_i and P_S are functions of t according to the trajectory of the source.

Adjustment of power allocation of each UAV and the source at every moment is too hard to implement. In order to reduce signaling overhead and implementation cost of dynamic power adjustment, we choose suitable T_S as the minimum changing unit of time. T_S can be properly adjusted according to the total motion time, engineering cost, hardware limitation and other targeted programmes. Taking T_S as a time interval, P_i and P_S can be dynamically adjusted to reduce SER with acceptable signaling overhead.

Furthermore, if the source's motion mode follows a certain pattern which can be easily predicted, the power allocation at each T_S can be configured or cached in the form of a list in power setting module of the source's and UAVs' transmission device in advance. Simulation results of the time-based power allocation will be presented clearly. In addition, within the range supported by the hardware, reducing T_S can improve the accuracy of the power adjustment that leads to better SER performance.

During the movement, the power of the source and the UAV switch dynamically according to the power allocation list, and in this way no signaling interaction is required. Through setting the list, we reckon that all devices can operate normally during power adjustment and utilize the allocated power efficiently for transmission. More detailed research on power headroom issues related to both remaining power and transmission power of the devices with corresponding power controls are well discussed in [24].

IV. PROBLEM FORMULATION OF SINGLE FOLLOWING UAV SCHEME

A. MULTI-HOP SIGNAL TRANSMISSION EXPRESSION

As is illustrated in Fig. 2, the system model of the single-UAV scheme is different from the multi-UAV scheme analyzed in Section II only in the number of UAV relay and the trajectory of movement. In view of that other parameters are the same, no repeated derivation and calculations are performed.

As mentioned in Section II, the existence of relative speed between the source and the single UAV leads to two situations.

On the one hand, when there is no relative speed between them, they move with the same trajectory all the time. d_{SR} of this scenario can be almost regarded as a constant c, however, d_{SR} is time-varying in the scheme in Section II according to the source's motion. So we can write other distance functions as follows:

$$d_{SD}(t) = \sqrt{\begin{array}{l}(X_B - X(t))^2 + (Y_B - Y(t))^2 \\ + (Z_B - Z(t))^2\end{array}} \tag{23}$$

$$d_{RD}(t) = \sqrt{\begin{array}{l}(X_B - X_R(t))^2 + (Y_B - Y_R(t))^2 \\ + (Z_B - Z_R(t))^2\end{array}} \tag{24}$$

The coordinate functions in (23) and (24) are determined by specific motion scenarios. Combining with specific triangles and geometric relationships like (12) and (13), these functions can be calculated so that we will not write it down in detail.

On the other hand, we assume that only during $0 - t_1$ can the UAV keep up with the source. However, the relative speed exists during $t_1 - t_2$, causing that the UAV can only try to follow the accelerating source. In this way, d_{SR} becomes variables again during $t_1 - t_2$. Therefore we have:

$$d_{SR}(t) = \begin{cases} \sqrt{\begin{array}{l}(X_R(t) - X(t))^2 \\ + (Y_R(t) - Y(t))^2, \\ + (Z_R(t) - Z(t))^2\end{array}} & t_1 \le t \le t_2 \\ constant\ c, & 0 \le t \le t_1 \end{cases} \tag{25}$$

In (25), these coordinate functions are determined by new scenario where the UAV cannot keep up with the source perfectly.

Regardless of the existence of relative speed between the following UAV and the source, in the first hop, y_{SD} is expressed in (4). y_{SR} can be written in the following form:

$$y_{SR} = \sqrt{P_S} \cdot \mathbf{H}_{SR} \cdot \mathbf{x} + n_{SR} \tag{26}$$

In the second hop, $\mathbf{y}_{RD}$ can be written as:

$$\mathbf{y}_{RD} = \lambda_1 \cdot \sqrt{P_1} \cdot \mathbf{H}_{RD} \cdot \mathbf{y}_{SR} + \mathbf{n}_{RD} \tag{27}$$

where λ_1 is calculated by (8).

B. CALCULATION OF SNR AND SER

Similarly, after unifying the noise of each link as n_{nor}, system SNR can be obtained as:

$$\gamma_{AF}^{MRC} = \gamma_{SD} + \gamma_{RD} \tag{28}$$

γ_{SD} denotes the SNR of the direct link in this scheme, and can be calculated by (9). In the meanwhile, γ_{RD}, on behalf of SNR of the relay link, can also be written as (10). Calculation of system SER is different from (16). The distribution it obeys can be written as:

$$f_\gamma(\gamma) = \theta_1\beta\left[\frac{e^{-\beta\gamma}}{(\theta_1-\beta)} - \frac{e^{-\theta_1\gamma}}{(\theta_1-\beta)}\right] \tag{29}$$

where β and θ_1 are defined in (14) and (15) respectively.

Based on (17), SER of this scheme with BPSK modulation can be finally obtained as:

$$P_{e_1} = \left(\frac{1}{2} - \frac{1}{2\sqrt{\beta+1}}\right)\cdot\frac{\theta_1}{(\theta_1-\beta)} - \left(\frac{1}{2} - \frac{1}{2\sqrt{\theta_1+1}}\right)\cdot\frac{\beta}{(\theta_1-\beta)} \tag{30}$$

In the same way, when the modulation order of PSK rises, we have:

$$P_{e_1}{}^{(N)} \approx 2\cdot\left[\begin{array}{l}\left(\frac{1}{2} - \frac{\sin(\frac{\pi}{N})}{2\sqrt{\beta+\sin^2(\frac{\pi}{N})}}\right)\cdot\frac{\theta_1}{(\theta_1-\beta)} \\ -\left(\frac{1}{2} - \frac{\sin(\frac{\pi}{N})}{2\sqrt{\theta_1+\sin^2(\frac{\pi}{N})}}\right)\cdot\frac{\beta}{(\theta_1-\beta)}\end{array}\right] \tag{31}$$

in which $N > 2$.

C. OPTIMIZATION FUNCTION OF SER AND POWER ALLOCATION STRATEGY

Similarly, the optimization function of SER can be obtained as:

$$\begin{aligned}\min_{P_s,P_1}\ & P_{e_1} = F(P_S, P_1)\\ & \mathrm{C1}: P_S + P_1 = P_t\\ \text{s.t. } & \mathrm{C2}: P_S > 0, P_1 > 0\\ & \mathrm{C3}: P_S < P_t, P_1 < P_t\end{aligned} \tag{32}$$

Through similar calculations in Section III, we can easily obtain that:

$$P_S = \frac{P_t}{1 + \frac{\sigma_{SR}^2}{\sigma_{RD}^2}\cdot\sqrt{\frac{|(\sigma_{RD}^2-\sigma_{SD}^2)|\cdot G_{SR}}{(G_{SD}\cdot\sigma_{SD}^2+G_{SR}\cdot\sigma_{SR}^2)}}} \tag{33}$$

P_1 denotes the transmit power of the single UAV, and the rest of P_t is assigned to it. Also, we have similar definition of $G_{SR}, G_{SD}, \sigma_{RD}^2, \sigma_{SR}^2, \sigma_{SD}^2$ that we have mentioned in Section III.

Different from the scheme in Section III, σ_{SR}^2 can be regarded as a constant in one stage, or it can be time-varying in another stage. Its features depend on whether relative speed exists between the source and the UAV relay.

Consistent with the multi-UAV scheme, the dynamic power allocation will be recorded as a list in units of T_S and can be set in the transmit devices of the source and the UAV if necessary.

V. SIMULATION RESULTS

In this section, the performance results of our proposed schemes are presented by simulation studies.

Adhering to the theme of ''Technological Winter Olympics'', we can effectively apply the above two types of UAV relay-assisted transmission schemes to related events of the Winter Olympics. In the following, we will adopt the motion scenario abstracted from practical tournament as a prototype to perform simulation verification. Certainly, our schemes can be extended to other similar moving scenes of communication fields. Here, we use ''individual skiing project'' as a prototype to abstract a type of motion model, the scene of which is consistent with Fig. 1. Several hovering UAV relays are arranged in advance for cooperative transmission. Since there are quite a lot of references to actual sports events, we can reasonably regard the source's movement as uniformly accelerating linear motion. Therefore, the motion time and source's trajectory are easy to predict. Considering the application criteria like the flying height standard and the safe distance against collision of UAV, in our simulated scenario, the number of hovering UAVs is limited to 2 or 3. According to the characteristics of the scenario, we determine the hovering position of each UAV that is more in line with the actual configuration in advance. Comparison and analysis of SER performance and power allocation strategy will be presented next.

In the multi-UAV relay schemes, the parameters of the system model are shown in Table.1. According to [26], (17) can be accurately calculated by the law of definite integration when BPSK is adopted. Whereas when the modulation order of PSK rises, we generally use approximate formula of (17) to obtain the expression of SER, which is presented in (21). Therefore, we take BPSK as signal modulation for accuracy in following simulations.

As mentioned in Section I, existing studies are mostly limited to single-antenna sources and UAVs. In the proposed schemes, M receive antennas are equipped at BS. Also, considering the carrying capacity of each UAV and the source's launcher, we adopt 2 antennas at transmitters of both the UAV and the source and 1 antenna at the UAV's receiver to get the diversity gain. In this section, 10^5 symbols are transmitted every second on each antenna of the source. Simulation in Fig. 4 shows that when dynamic power allocation strategies are adopted, our multi-antenna relay system outperforms those traditional schemes with single antenna. In view of the practical configuration problems and stability, we will simulate and analyze with $M = 8$, as shown in Table.1.

We simulate both the real-time SER and mean SER of the whole motion process under different system power limitations to evaluate our proposed schemes. It is worth noting that mean SER denotes the average of the SER at each T_S during the whole motion that lasts for $t_2 = 24$s. We adopt fixed power allocation scheme in [6] and power allocation of IHDAF in [27] as comparison. As for scheme in [6], $\delta_1 P_t$ denotes the fixed power of the source, in which δ_1 denotes the fixed power allocation factor and $(1-\delta_1)P_t$ is

TABLE 1. Parameters of multi-UAV relay schemes.

Symbol	Parameter Name	Value
θ	slope	30°
H	vertical drop	100m
L	horizontal length	170m
L_A	slope length	200m
σ^2	noise variance	-104dBm
α	fading factor	3
t_2	the whole motion time	24s
T_S	minimum changing unit of time	1s
P_t	system power limitation	0.2W
$H_{R\max}$	maximum flying height of UAV	120m
$V_{R\max}$	maximum flying speed of UAV	27m/s
(X_B, Y_B, Z_B)	coordinates of the remote BS	(500,500,25)m
M	number of receive antennas at BS	8
a	acceleration of the source	$0.64\mathrm{m/s^2}$
$\left[X_{R_1}^{(2)}, 0, Z_{R_1}^{(2)}\right]$	location of the first UAV in 2-UAV scheme	(30,0,90)m
$\left[X_{R_2}^{(2)}, 0, Z_{R_2}^{(2)}\right]$	location of the second UAV in 2-UAV scheme	(100,0,50)m
$\left[X_{R_1}^{(3)}, 0, Z_{R_1}^{(3)}\right]$	location of the first UAV in 3-UAV scheme	(30,0,70)m
$\left[X_{R_2}^{(3)}, 0, Z_{R_2}^{(3)}\right]$	location of the second UAV in 3-UAV scheme	(90,0,50)m
$\left[X_{R_3}^{(3)}, 0, Z_{R_3}^{(3)}\right]$	location of the third UAV in 3-UAV scheme	(150,0,20)m

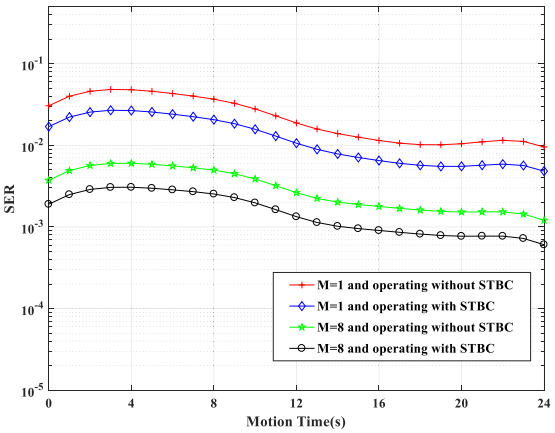

FIGURE 4. SER of different applications of multi-antenna technology in 3-UAV scheme when *M*=1 or 8 and whether STBC is adopted.

allocated to one UAV relay. Even if there are multiple UAVs in the scenario, only one UAV with the best channel conditions participates in the relay transmission and can utilize the fixed power in different periods of the whole motion, while other UAVs are not working. According to the locations of 3 or 2 hovering UAV relays, we adopt (14, 20, 24) and (17, 24) as time-splitting points of 3-UAV scheme and 2-UAV scheme. In detail, during 0 – 14s, 14 – 20s and 20 – 24s, 3 UAV relays work in turn. Similarly, during 0 – 17s and 17 – 24s, 2 UAV relays work in turn. In this scheme δ_1 is fixed as 0.5.

As for power allocation in IHDAF proposed in [27], the optimal power allocation factor δ_2 is selected based on

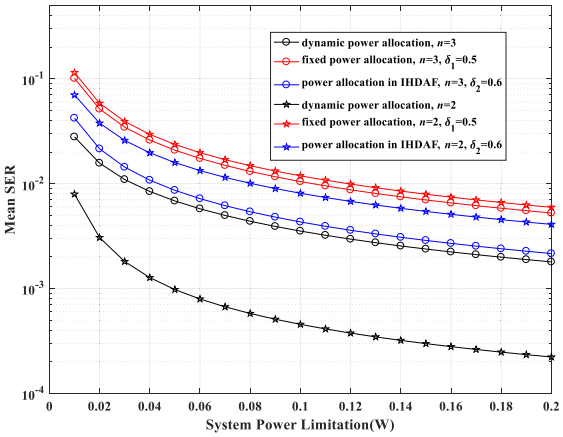

FIGURE 5. Mean SER under different total power limitations when $n = 2$ or 3 and with different power allocation strategies.

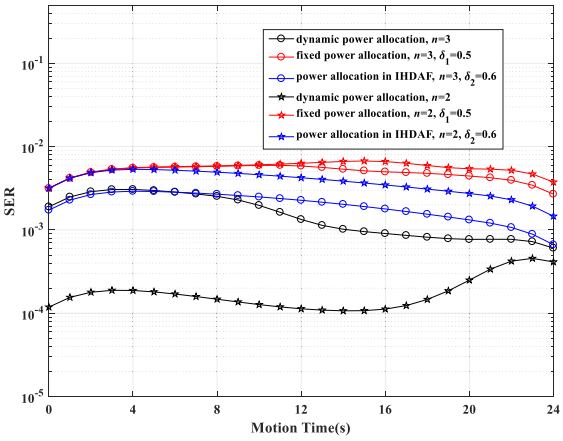

FIGURE 6. Real-time SER when $n = 2$ or 3 and with different dynamic power allocation strategies($P_t = 0.2$W).

the relative size of d_{SR_i} and d_{R_iD} after normalization. Finally the optimal δ_2 is selected as 0.6 according to our scenario in Fig. 1 and the results in [27]. All the hovering UAV relays work simultaneously with different power. $\delta_2 P_t$ is allocated to the source, and the remaining power is allocated to the UAVs. Taking into account their different locations in our scenario as well as the relationship between the normalized size of d_{SR_i},d_{R_iD} and their power allocation in [27], in 3-UAV scheme, $(1 - \delta_2)P_t$ is allocated to 3 UAVs with the ratio of 6:8:11, whlie in 2-UAV scheme, it is alloated to 2 UAVs with another ratio of 2:3.

As can be seen in Fig. 5, increasing the total power of the limited system can reduce the mean SER in our scenario. So in Fig. 6, we take P_t as 0.2W. In addition, we note that whether there are 3 or 2 hovering UAV relays, the real-time SER of dynamic power allocation scheme is lower than that of fixed power allocation and IHDAF. Lack of reasonable adjustments to UAV's power according to the changes in the motion state of the source may lead to this phenomenon. In addition, when $n = 3$, IHDAF is closed to our scheme, but when $n = 2$, its SER performance becomes much worse.

Unexpectedly, the 2-UAV relay system with dynamic power allocation can significantly improve the system

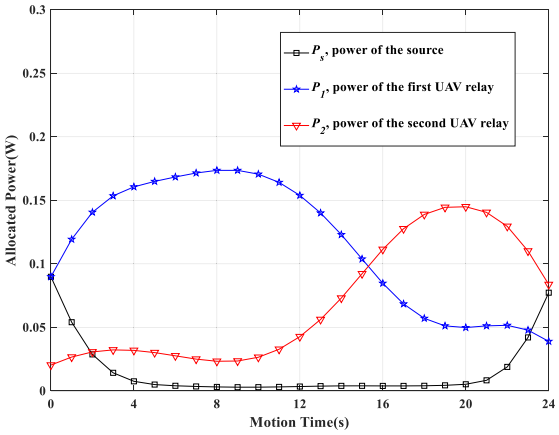

FIGURE 7. The real-time dynamic power allocation strategy of each end in 2-UAV relay system.

performance, whereas, performance of the 3-UAV relay system slightly improves. Also, with our power allocation strategy, the 2-UAV scheme performs better than that of the 3-UAV scheme. However, we often reckon that more relays can provide more additional links to increase the quality of cooperative transmission. In fact, since the total power is limited, the more UAVs gain the better performance at the beginning because of diversity, but when the number of UAVs increases, the assigned power of each UAV decreases accordingly, instead resulting in the deterioration of the quality of each link and limiting the performance of the entire system.

In addition, in our scheme, the trajectory of the moving source actually leads to a certain ''correlation'' among different relay links. This correlation exists mathematically because our power allocation is related to $d_{SR_i}, d_{SD}, d_{R_iD}$, which are time-varying functions highly related to the source's trajectory. Excessive channel correlation also leads to performance degradation. In this way, we conclude that in specific motion scenarios, more is not always the better for the number of UAV relays. Therefore, there is an optimal number of hovering UAVs for each scenario. Exceeding this amount may lead to the deterioration of the system's quality.

Besides SER performance, we also focus on dynamic power allocation in our proposed scheme. Since 2-UAV system is more suitable for our scenario, its real-time power allocation strategy is illustrated by Fig. 7. As in the prototype of individual skiing project, there are obstacles like mountains between the source and the remote BS, so the system tries to avoid allocating more power to the direct link because of poor channel conditions, that's why P_S is small for a long time. Since the UAV relays are sequentially passed by the source, in different periods, each UAV relay is assigned to maximum power in sequence, and two peaks appear in curves of P_1 and P_2 respectively. It is worth noting that the source will not be allocated so little power in every scenario. If it is close enough to BS, the direct link will be allocated a considerable amount of power. At the beginning and in the end of the motion, P_S has picked up. It can be explained as follows: at the beginning of the movement, due to the high initial position and less obstruction, the channel condition of the direct link is sufficient to obtain higher power. With the rapid decline in altitude, it drops sharply, resulting in a rapid decrease of P_S. Near the end of the motion, the system will try to increase P_S to the second UAV because it is reliable enough to ensure the performance of the system.

TABLE 2. Special parameters of single-UAV relay scheme.

Symbol	Parameter Name	Value
$[X_{R_0}(t), 0, Z_{R_0}(t)]$	initial position of the following UAV	(0,0,120)m
$[X_0(t), 0, Z_0(t)]$	initial position of the source	(0,0,100)m
d_{SR}	distance between source and UAV with no relative speed appears	20m
$V'_{R\max}$	the maximum speed of UAV when relative speed appears	5m/s
t_1	the time when the relative speed started to appear	8s

The overall trend of the curves in Fig. 7 is as follows: limited by the environment and the transmitting device, P_S is always small except the beginning and the end of the motion, P_1 and P_2 alternately have maximum power allocation, which is consistent with each UAV's location. According to C1 in (20), the total power of the source and 2 UAVs are limited as P_t due to our proposed extreme communication scenario. Compared to stationary relays, the height and 3D placement of UAV relays provide more links with better conditions to amplify and forward the signal, therefore, when they are allocated relatively more power within the given limitation, we will obtain better SER performance. To some extent, by introducing UAV relays, the limited system power has been most effectively used.

As for the simulations of single-UAV relay system, most parameters of the scenario are the same with those of multi-UAV relay system, which are listed in Table.1, so we only list the different parameters in Table.2.

Two kinds of situations are simulated. For one, during the whole motion process, the single UAV follows the source perfectly. Their trajectories are almost the same, so their distance d_{SR} keeps as a constant. For another, our UAV is influenced by the extreme natural environment or limited by hardware and other potential problems. In fact, this situation is common in practical scenario. As a result, during the period of $0 - t_1$, the UAV follows the source with uniformly accelerated movement. However, it reached its maximum speed $V'_{R\max}$ at t_1 and after that moment, the UAV flies at the same speed, whereas, the source is still accelerating. Accompanied with the emergence of relative speed, d_{SR} now becomes a time-varying function which can be calculated according to the scenario.

Ideologically the same as the multi-UAV relay systems, we reckon that with proposed dynamic power allocation strategy, the single-UAV relay system has better performance of SER because the compared schemes do not consider the

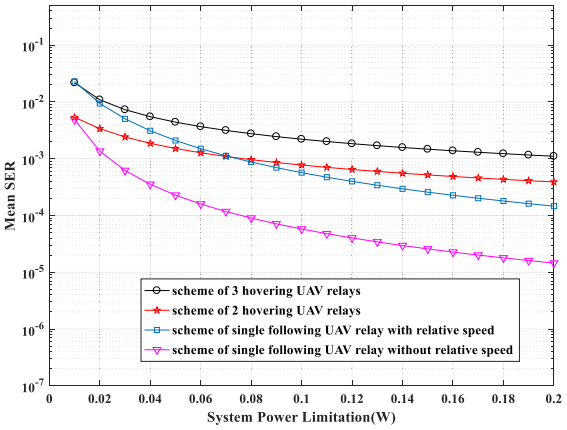

FIGURE 8. Mean SER of multi-UAV relay systems when $n = 2$ or 3 and single-UAV relay system (whether relative speed exists) under different system power limitations.

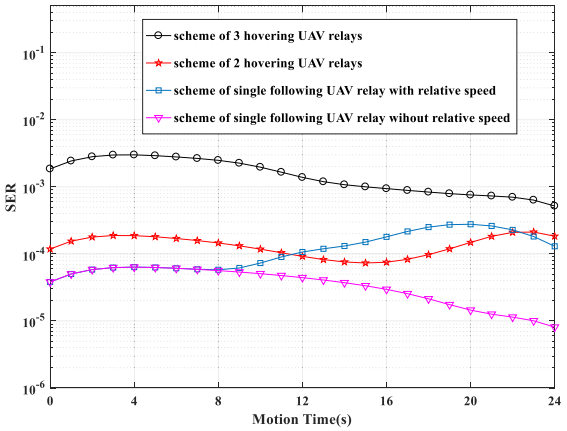

FIGURE 9. SER of multi-UAV relay systems when $n = 2$ or 3 and single-UAV relay system (whether relative speed exists) during the whole motion process ($P_t = 0.2$W).

co-movement of the source and the UAV. So in following simulations, dynamic power allocation strategy is always adopted. We pay more attention to the performance compared with that of multi-UAV relay schemes in the same scenario. Besides, the impact on SER and power allocation, caused by relative speed between the source and the UAV, will be shown.

Fig. 8 shows that as system power increases, regardless of the existence of relative speed, the mean SER of the single-UAV relay scheme will reduce. Without relative speed, the single following UAV brings a visible lower SER of the system. Even with relative speed, this scheme is also slightly better than the schemes with 2 UAVs that we mentioned before. We can conclude that the single following UAV effectively exerts its maneuverability, which brings better transmission performance in this scenario.

Fig. 9 shows the real-time SER of the schemes above. As we assumed, relative speed appears when $t_1 = 8$s so that the SER curves of these two cases begin to diverge. As the distance between the UAV and the source increases, SER of the scheme with relative speed is getting worse compared with the case that the UAV always keeps up with the source. Also we can notice that on the second half of the motion

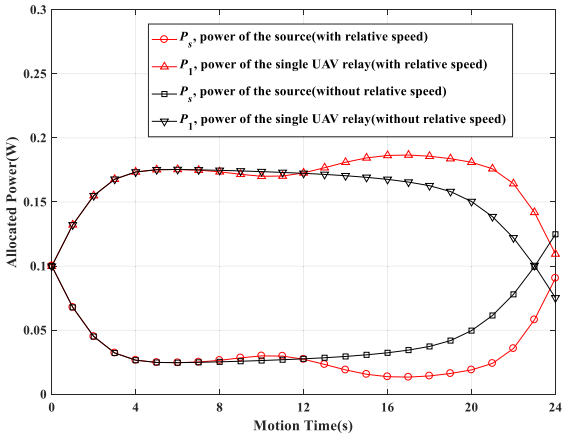

FIGURE 10. The real-time power allocation of the source and UAV in single-UAV relay system:comparison of two situations whether relative speed exists or not.

process, SER performance of the single-UAV scheme with relative speed is close to that of the 2-UAV scheme. Considering that the situation with no relative speed is ideal, even if it has the best performance, we sitll focus more on the situation with relative speed. This situation can be extended to a variety of practical problems such as insufficient UAV battery life, system failure, and hardware limitations, so it has more research significance. In summary, in our proposed scenario, if ideal, the perfectly following single-UAV relay system has the best transmission performance. Otherwise, the single-UAV scheme with relative speed and the 2-UAV scheme have similar performance.

Fig. 10 clearly shows the different dynamic power allocation of these two situations. Likewise, divergence appears when $t_1 = 8$s. We notice that without relative speed, the power allocation of the system is more balanced, especially in the second half of the entire motion. Conclusion can be drawn that our dynamic power allocation strategy independently increases the forwarding power of the UAV in order to compensate the signal transmission quality because the source is getting farther. So our scheme with dynamic power allocation is more flexible with self-adjusting ability.

In summary, no matter there are several hovering UAVs or just only single following UAV, our schemes based on multi-antenna technology and dynamic power allocation obtain better SER performance. With different values of T_S, the power allocation strategy can be input into the power transmitter of the source and the UAVs in advance to reduce signaling overhead. In extreme communication scenarios, simulations show that our schemes can be self-adjusting according to different conditions. The schemes with multiple hovering UAVs or single following UAV can be chosen according to specific motion scenarios and other restrictions, like cost, implement difficulty, UAV criterion, etc.

VI. CONCLUSION

In this article, we have designed two UAV-assisted AF relaying schemes for high-speed moving sources, including

multiple hovering UAVs and single following UAV. Firstly, typical motion models are proposed for the two schemes respectively. And then, according to the trajectories of the moving source and the UAVs, as well as the time-varying channels which are highly related to them, we have derived the SER expressions of each scheme. After operating SER minimization, we have obtained the dynamic power allocation strategies which can cope well with source's motion state compared with existing ones. Finally, verified by simulations, our schemes with dynamic power allocation have better SER performance than that of the compared schemes. Self-adjusting ability of power allocation makes our schemes more flexible in practical engineering. Simulations also show that our schemes can be chosen purposefully according to specific engineering requirements, helping find the most suitable UAV relay strategy with excellent performance.

REFERENCES

[1] D. E. Simmons and J. P. Coon, "Two-way OFDM-based nonlinear amplify-and-forward relay systems," *IEEE Trans. Veh. Technol.*, vol. 65, no. 5, pp. 3808–3812, May 2016.

[2] P. Kumar and K. Dhaka, "Performance analysis of a decode-and-forward relay system in κ-μ and η-μ fading channels," *IEEE Trans. Veh. Technol.*, vol. 65, no. 4, pp. 2768–2775, Apr. 2016.

[3] Y. Liu, G. Pan, H. Zhang, and M. Song, "Hybrid decode-forward & amplify-forward relaying with non-orthogonal multiple access," *IEEE Access*, vol. 4, pp. 4912–4921, Aug. 2016.

[4] K. G. Seddik, A. K. Sadek, W. Su, and K. J. R. Liu, "Outage analysis of multi-node amplify-and-forward relay networks," in *Proc. IEEE Wireless Commun. Netw. Conf. (WCNC)*, vol. 2, Apr. 2006, pp. 1184–1188.

[5] S.-I. Chu, "Outage probability and DMT performance of underlay cognitive networks with incremental DF and AF relaying over Nakagami-m fading channels," *IEEE Commun. Lett.*, vol. 18, no. 1, pp. 62–65, Jan. 2014.

[6] P. Kumar and K. Dhaka, "Average BER and resource allocation in wireless powered decode-and-forward relay system," *IET Commun.*, vol. 13, no. 4, pp. 379–386, Mar. 2019.

[7] X. Liu and W. Du, "BER-based comparison between AF and DF in three-terminal relay cooperative communication with BPSK modulation," in *Proc. 12th Int. Conf. Mobile Ad-Hoc Sensor Netw. (MSN)*, Dec. 2016, pp. 296–300.

[8] D. Qin and Y. Wang, "BER minimization for AF relay-assisted OFDM systems," *IEEE Commun. Lett.*, vol. 19, no. 3, pp. 495–498, Mar. 2015.

[9] T. T. Duy and H.-Y. Kong, "Performance analysis of hybrid decode-amplify-forward incremental relaying cooperative diversity protocol using SNR-based relay selection," *J. Commun. Netw.*, vol. 14, no. 6, pp. 703–709, Dec. 2012.

[10] D.-B. Ha, D.-D. Tran, D.-H. Ha, and A.-N. Nguyen, "Improving network performance by using multiple power-constrained amplify-and-forward relays," in *Proc. Int. Conf. Inf. Netw. (ICOIN)*, 2017, pp. 231–235.

[11] D. Hwang, S. S. Nam, T.-J. Lee, and D. I. Kim, "Finite feedback MIMO precoding for the two-way Amplify-and-Forward relay network," *IEEE Commun. Lett.*, vol. 18, no. 4, pp. 620–623, Apr. 2014.

[12] J. Sharma and Y. P. K. Sarma, "BER performance analysis of cooperative MIMO system with two-way relay using physical network coding," in *Proc. 11th Int. Conf. Ind. Inf. Syst. (ICIIS)*, Dec. 2016, pp. 518–522.

[13] X. Song and S. Xu "Joint optimal power allocation and relay selection in full-duplex energy harvesting relay networks," in *Proc. Int. Conf. Commun. Softw. Netw. (ICCSN)*, Jul. 2018, pp. 80–84.

[14] J. Shen, Y. Liu, H. Yang, and C. Yan, "Joint time allocation and power splitting schemes for Amplify-and-forward relaying network over log-normal fading channel," in *Proc. 10th Int. Conf. Wireless Commun. Signal Process. (WCSP)*, Oct. 2018, pp. 1–5.

[15] V. Sharma, M. Bennis, and R. Kumar, "UAV assisted heterogeneous networks for public safety communications," *IEEE Commun. Lett.*, vol. 20, no. 6, pp. 1207–1210, Jun. 2016.

[16] H. He, S. Zhang, Y. Zeng, and R. Zhang, "Joint altitude and beamwidth optimization for UAV-enabled multiuser communications," *IEEE Commun. Lett.*, vol. 22, no. 2, pp. 344–347, Feb. 2018.

[17] S. Shakoor, Z. Kaleem, D.-T. Do, O. A. Dobre, and A. Jamalipour, "Joint optimization of UAV 3D placement and path loss factor for energy efficient maximal coverage," *IEEE Internet Things J.*, early access, Aug. 24, 2020, doi: 10.1109/JIOT.2020.3019065.

[18] N. Zhao, F. Cheng, F. R. Yu, J. Tang, Y. Chen, G. Gui, and H. Sari, "Caching UAV assisted secure transmission in hyper-dense networks based on interference alignment," *IEEE Trans. Commun.*, vol. 66, no. 5, pp. 2281–2294, May 2018.

[19] F. Cheng, G. Gui, N. Zhao, Y. Chen, J. Tang, and H. Sari, "UAV-relaying-assisted secure transmission with caching," *IEEE Trans. Commun.*, vol. 67, no. 5, pp. 3140–3153, May 2019.

[20] S. Shakoor, Z. Kaleem, M. I. Baig, O. Chughtai, T. Q. Duong, and L. D. Nguyen, "Role of UAVs in public safety communications: Energy efficiency perspective," *IEEE Access*, vol. 7, pp. 140665–140679, Sep. 2019.

[21] N. Goddemeier, K. Daniel, and C. Wietfeld, "Role-based connectivity management with realistic air-to-ground channels for cooperative UAVs," *IEEE J. Sel. Areas Commun.*, vol. 30, no. 5, pp. 951–963, Jun. 2012.

[22] J. Zhang, Y. Zeng, and R. Zhang, "Spectrum and energy efficiency maximization in UAV-enabled mobile relaying," in *Proc. IEEE Int. Conf. Commun. (ICC)*, May 2017, pp. 1–6.

[23] J. Xu, Y. Zeng, and R. Zhang, "UAV-enabled multiuser wireless power transfer: Trajectory design and energy optimization," in *Proc. Asia–Pacific Conf. Commun. Bridg. Metrop. Remote (APCC)*, Dec. 2017, pp. 1–6.

[24] W. Kim, Z. Kaleem, and K. Chang, "Power headroom report based uplink power control in 3GPP LTE-A HetNet," *EURASIP J. Wireless Commun. Netw.*, vol. 2015, no. 6, pp. 1–13, Dec. 2015.

[25] B. Ji, Y. Li, B. Zhou, C. Li, K. Song, and H. Wen, "Performance analysis of UAV relay assisted IoT communication network enhanced with energy harvesting," *IEEE Access*, vol. 7, pp. 38738–38747, Mar. 2019.

[26] J. Zheng, J. Zhang, S. Chen, H. Zhao, and B. Ai, "Wireless powered UAV relay communications over fluctuating two-ray fading channels," *Phys. Commun.*, vol. 35, Aug. 2019, Art. no. 100724.

[27] Z. Bai, J. Jia, C. Wang, and D. Yuan, "Performance analysis of SNR-based incremental hybrid decode-amplify-forward cooperative relaying protocol," *IEEE Trans. Commun.*, vol. 63, no. 6, pp. 2094–2106, Jun. 2015.

[28] T. M. Duman and A. Ghrayeb, *Coding for MIMO Communication Systems*. London, U.K.: Wiley, Oct. 2007, pp. 24–25.

[29] S. Shulong, "On distribution of sums of n independent random variables subject to exponential distribution," (in Chinese), *J. Liaoning Normal Univ.*, vol. 4, no. 4, pp. 51–58, Apr. 1990.

[30] M. L. Ulrey, "Formulas for the distribution of sums of independent exponential random variables," *IEEE Trans. Rel.*, vol. 52, no. 2, pp. 154–161, Jun. 2003.

[31] G. P. John and S. Masoud, *Digital Communications*, 5th ed. New York, NY, USA: McGraw-Hill, 2008, pp. 192–194 and 1100–1103.

JI WU received the B.S. degree in communication engineering from the Beijing University of Posts and Telecommunications (BUPT), Beijing, China, in 2018, where he is currently pursuing the M.S. degree in information and communication engineering with the State Key Laboratory of Networking and Switching Technology.

His current research interests include MIMO and massive MIMO, UAV techniques, and coordinated transmission and the combination of them.

LIHUA LI (Member, IEEE) received the B.E. and Ph.D. degrees from the Beijing University of Posts and Telecommunications (BUPT), Beijing, China, in 1999 and 2004, respectively. She was a Visiting Scholar with the University of Oulu, Oulu, Finland, from August 2010 to August 2011, and Stanford University, CA, USA, from April 2015 to April 2016. She is currently a Professor with BUPT. Her research focuses on wideband mobile communication technologies, including MIMO and massive MIMO, cooperative transmission technologies, link adaptation, and so on; and relating to new generation mobile communication systems, such as 5G and beyond. She has published 95 papers in international and domestic journals and academic conferences and five books. She has applied 23 national invention patents and one international patent. She was selected and funded as one of the New Century Excellent Talents by the Chinese Ministry of Education, in 2008. She won the Second Prize of the State Technological Invention Award (top-3 China national awards), in 2008, and the First Prize of the China Institute of Communications Science and Technology Award, in 2006, for research achievements of Wideband Wireless Mobile TDD-OFDM-MIMO Technologies.

LIUTONG DU (Student Member, IEEE) received the B.Sc. degree in communication engineering from the Beijing University of Posts and Telecommunications (BUPT), Beijing, China, in 2014, and the M.Sc. degree in electronic and communication engineering from the State Key Laboratory of Networking and Switching Technology, BUPT, in 2017, where he is currently pursuing the Ph.D. degree.

His current research interests include MIMO and massive MIMO, non-linear precoding techniques, and physical-layer security and the combination of them.